3D INTERFACE ELEMENTS FOR MODELING COMPLEX POTENTIAL DROPS - COMPARISON WITH A BOUNDARY ELEMENTS METHOD

Valéry Poulbot, Laurent Krähenbühl, Philippe Massé, R. Blanpain

▶ To cite this version:

HAL Id: hal-00140684

https://hal.archives-ouvertes.fr/hal-00140684

Submitted on 25 Apr 2007

3D Interface Elements for Modelling Complex Potential Drops. Comparison with a Boundary Elements Method.

Valéry Poulbot[1][2], Laurent Krähenbühl[2], Philippe Massé[1][3], Roland Blanpain[1]

[1]LETI (CEA - Technologies avancées) - CENG, 17 rue des Martyrs, 3805 Grenoble Cedex 9 (France)

[2]Centre de Génie Electrique de Lyon - URA CNRS 829 - ECL, BP 163, 69131 Ecully Cedex (France)

[3]Laboratoire MADYLAM - ENSIEG INPG - BP 95, 38402 Saint-Martin-d'Hères Cedex (France)

Abstract—Voltage drops due to complex surface impedance and/or surface current sources are modelled by a 3D Finite Elements Method. Two specific formulations are given with these special 3D curvilinear second order elements : conduction in a low frequency marine electrometer and thermoelectric Seebeck effect on a solidification front. Simultaneous normal and tangential interfacial discontinuities can be computed. The method is validated by comparison with a Boundary Elements Method and experimental values.

I. INTRODUCTION

There are many physical problems in which the variable is discontinuous at the boundary between two media. In the Finite Element Method, the drop of the normal component of the gradient of a continuous state variable is a natural boundary condition, but the drop of the state variable itself or the drop of the normal *and* tangential components of its gradient must be computed with a special procedure. We have developed and implemented a general first and second order, 2D and 3D, interface finite element in the FLUX-EXPERT® [1, 2] package in order to take into account such surface properties and discontinuous variable. A FEM model with special elements is compared with a BEM model described with the PHI3D® software [3]. Similar results are obtained with both methods.

The first application solves the electrochemical problem of the drop voltage at the interface of an electrode and an electrolyte with a surface complex impedance. The aim of this development is to model a low frequency marine electrometer in its environment [4]

The second application computes the drop of the pseudo-electric potential produced by the thermoelectric Seebeck effect at the interface of solidification of binary alloys. The aim of this development is to model the electric current generated in the vicinity of a microscopic model dendrite on a solidification front [5].

II. PRINCIPLE

The general interfacial element is a couple of second order classic 3D elements linked by a second order classic boundary element (Fig. 1).

The various cases have been developed in 2D : square and triangle (segment) and in 3D : cube, prism (square) and prism, tetrahedron (triangle).
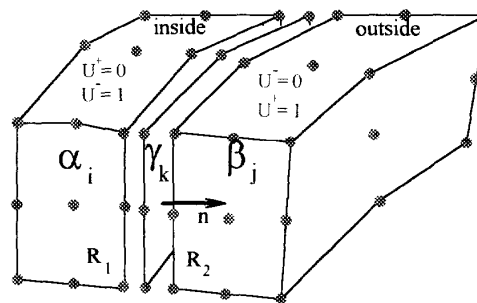

Fig. 1: The general interfacial element

On such an element three sets of polynomial are computed α_i, β_j and γ_k for each element part. Their gradients must be computed according to the curvilinear isoparametric transformation given by the interface part of the element : γ. The normal and tangential vectors are needed on each point of this interface.

The interface equations must be projected on the basis given by the γ_k functions.

The integration can be performed with a Gauss Legendre Technique with integration points computed on the boundary part of the element (3x3 points have been used for squares, 7 for triangles, 3 for segments).

These kinds of elements are built by a special program which compresses an initial 2nd order mesh in the area of the discontinuity. With such a technique, the discontinuity can begin and end inside the computation domain, without any trouble at the extremity where partially compressed elements are automatically built. (The example of the electrometer uses such elements between the end of the electrodes and the environment).

III. EXAMPLE 1 : SURFACE IMPEDANCE MODEL

At very low frequency in a conducting media, the very classic equation must be solved.

$$\vec{\nabla}(-\sigma\vec{\nabla}\Phi) = 0 \qquad (1)$$

where σ is the (complex) electrical conductivity and Φ the unknown complex electrical potential. In such a case with a standard FE formulation, classic integrant A must be computed:

$$A = \iiint \sigma\vec{\nabla}W_i\vec{\nabla}W_j dxdydz \qquad (2)$$

The classic boundary condition at the interface between two materials without electrochemical effect verifies :

$$\sigma_2\vec{\nabla}\Phi_2 \cdot \bar{n} = \sigma_1\vec{\nabla}\Phi_1 \cdot \bar{n} \quad (= \vec{J}\cdot\bar{n}) \qquad (3)$$

But on an electrochemical interface, the current must be :

$$\sigma_S(\Phi_2 - \Phi_1) = \vec{J}\cdot\bar{n} \qquad (4)$$

where σ_S is the interfacial surface conductivity :

$$\sigma_S = 1/\underline{Z} \,. \, S = \sigma_3/2\varepsilon \qquad (5)$$

$\underline{Z}$ is the (measured) electrode impedance, S the electrode surface in contact with the electrolyte, σ_3 is the volume conductivity and 2ε the thickness of the interface.

In order to compute A (Eq. 2) in this interface, two kinds of computations can be done : the interface has a very small but non zero thickness (2ε), or the thickness is zero.

In the first case, it must be assumed that :

H_1: The variation of the potential is linear on the normal direction.

H_2: The tangential variation of the potential is free in the interfacial element.

In such a case, the classic term can be integrated analytically by :

$$A = \iint_S \left[\int_{-\varepsilon}^{+\varepsilon} \sigma_3 \frac{\partial}{\partial w}W_i \cdot \frac{\partial}{\partial w}W_j \, dw \right] \cdot ds \qquad (6)$$

in which :

$$W_i = \frac{1}{2}(1\pm\frac{w}{\varepsilon})\gamma_i(u,v) \qquad (7)$$

(+) if $i \in$ outside part of the boundary.

(−) if $i \in$ inside part of the boundary.

$\gamma_i(u,v)$: Lagrange polynomial on the boundary (fig. 1)

After integration and with (Eq. 5) :

$$A = \pm\iint_S \sigma_S\gamma_i(u,v)\gamma_j(u,v)dudv \qquad (8)$$

positive sign if i and j are on the same side of S

In the second case, ε is equal to zero, the H_1 and H_2 hypotheses are not necessary : however, the test functions used in the finite element formulation have to be discontinuous on the interface. Such functions are built from the standard (continuous) tests functions W_i by using the *region unit functions* U_S^+ and U_S^- : U_S^+ is 0 inside S, and 1 outside, and reciprocally:

$$W_j \rightarrow \begin{cases} W^+ = W_j \cdot U_S^+ \\ W^- = W_j \cdot U_S^- = 1 - W^+ \end{cases} \qquad (9)$$

Because of the $U_S^\pm$ functions, the derivatives of W^+ and W^- contain Dirac's surface pulses $\delta(S)\cdot\bar{n}$:

$$\vec{\nabla}W^\pm = \vec{\nabla}(U_S^\pm \cdot W_j) = U_S^\pm \cdot \vec{\nabla}W_j \pm \gamma_j\cdot(\delta_S\bar{n}) \quad (10)$$

which only will give a non-null value to the integral A (Eq. 2) in the (null) volume of the interface. Using the general properties of δ:

$$\int_\mathcal{V} f\cdot\delta_P\cdot dV = f(P) \quad \text{with:} \quad f = \sigma_S\cdot(\Phi_2 - \Phi_1) \qquad (11)$$

we get: $\qquad (12)$

$$\iiint_\mathcal{V} \sigma_S(\Phi_2 - \Phi_1)\vec{\nabla}W^\pm\cdot dv = \pm\iint_S \sigma_S(\Phi_2 - \Phi_1)\gamma_j\cdot\bar{n}ds$$

After discretization, we find again the previous result (Eq. 8).

IV. APPLICATION: LOW FREQUENCY MARINE ELECTROMETER

Measurement of ultra low frequency (ULF : range 10^{-3} to 5 Hz) electric fields in the sea is of great interest for many scientific subjects, such as physical oceanography, geophysics, submarine detection or offshore industry. In a general way, oceanic signals from natural or artificial electric fields are very low (about 10^{-9} V/m), and high sensitivity of the recording instrumentation is required [6].

The most usual measurement technique consists in measuring the voltage between two contact points with the sea water (electrodes). This gives the electric field value along the direction of a line between the two electrodes, after dividing by the separation distance. Practical implementation of this method has given a large number of different devices, in relation with the origin and the frequency range of the field to be measured. An extended review of ULF electromagnetic fields in the sea and associated instrumentation is given in [4].

A new method was recently proposed , based on a current density measurement [7, 8]. Electric field in the sea arise as a result of electric current flowing through the water, according to the Ohm's law in conducting media :

$$\vec{J} = \sigma\vec{E} \qquad (13)$$

where σ is the sea water conductivity.

The volume current density is collected on large plane electrodes, between them a lineic current is measured, which depends on the surface of the electrodes. In order to not disturb the electric field lines, the global impedance of the measurement device must be suited (at ULF frequencies) to the equivalent impedance of the replaced water volume in the measurement direction. So this technique allows to take all the energy of the signal. Fig. 2 shows the two methods comparatively.

tension type electrometer

$$E = -V/L$$

$$I = j \cdot S \qquad E = I/\sigma S$$
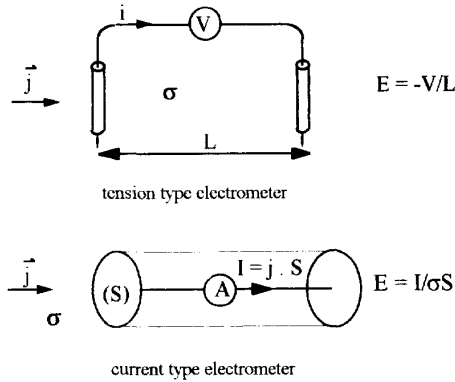
current type electrometer

Fig. 2. Electric field measurement methods

We have developed and build a *current collection* based marine electrometer, with a original current measurement system [9] and special design electrodes. Details of the prototype and different steps of its performing are described in [4]. The grading of the electrometer was made in laboratory in a basin with artificial sea water. The test bed is showed on Fig. 3. The apparatus has a cylindrical grading and disk electrodes. Two subsidiary electrodes (injection electrodes) put on either internal side of the basin allow to impose known electric field.
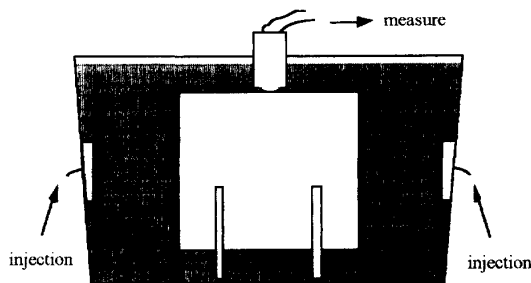

Fig. 3. Marine electrometer in the test basin

Satisfactory results are obtained with the first prototype, which has a self noise level about 10^{-9} V/m/H$^{-1/2}$. However, some improvement are even possible. In order to optimise the next prototype without a lot of new experimentations, we have performed 2D and 3D numerical models of the sensor in the basin.

Because of the impedance suiting criterion, the impedance of the (reception) electrodes, which is a function of the electrolyte exposed surface and a large number of physical and chemical parameters, has a great importance for the sensitivity of the apparatus and the calculation of its transfer function. Furthermore, this impedance induces a voltage between the microscopic interface electrode - electrolyte, and so a signal loss for the measure. We have identified from impedance measurements an equivalent circuit model for the interface electrode-electrolyte (Fig. 4).

For the simulations, we use this model (electrosorption impedance) with the parameters C_{dc} = 0.21F, C_{ads} = 0.83F, R_t = 0,97Ω, and S = 2325cm^2.
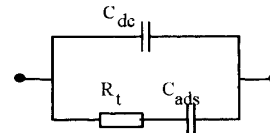

Fig. 4. Circuit model for the electrolyte /electrode interface

V. ELECTROMETER MODEL AND FEM RESULTS

We use for the FEM model equations of III. 2D and 3D modelisation are performed. Vertical slide of the geometry which is used for the 2D calculations is showed Fig. 5.
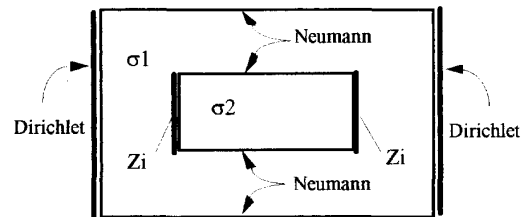

Fig. 5. Boundary conditions (FE and BIE Models)

The electrode interfaces in which the potential is rapidly varying are extremely thin (about 10^{-10}m). Electrode interfaces are so geometrically described with interfacial elements (zero thickness) and an equivalent surface conductivity (Eq. 5) corresponding to the impedance model of Fig. 4 and the previously exposed parameters.

The impedance of the internal current detection circuit is inductive. For the numerical FEM simulation, this impedance is modelled by an equivalent volume conductivity:

$$\sigma_2 = L/(Z_2 S)$$

where:

$$L = 0,684cm, \ S = 0.2325cm^2 , \ Z_2 = 0,73+j\omega 0.0194 \ \Omega$$

The conductivity of the electrolyte is $\sigma_1 = 4\Omega m^{-1}$, representative of natural sea water.

The casing of the electrometer is described with interfacial elements and a zero surface conductivity. Boundary conditions are those of Fig. 5.

2D and 3D simulations are perform with those parameters and frequencies ranging 10^{-3} to 10 Hz. In 3D, only a quarter of the geometry is describe in order to reduce the number of unknowns. The following figures (6 and 7) show respectively 2D and 3D calculated electric potential at frequency of 1 Hz.
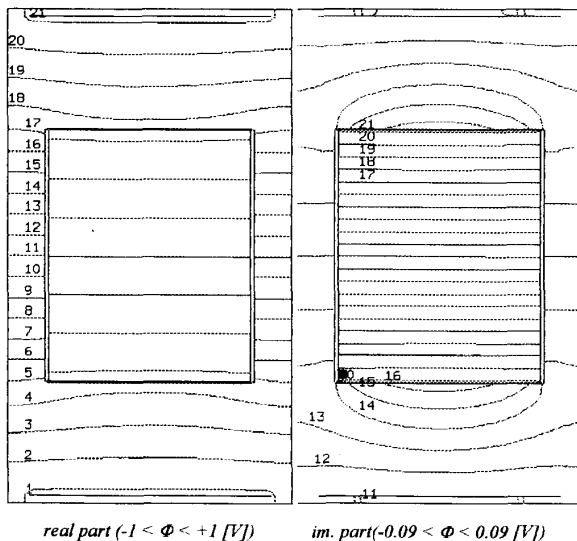

real part (-1 < Φ < +1 [V])   *im. part(-0.09 < Φ < 0.09 [V])*

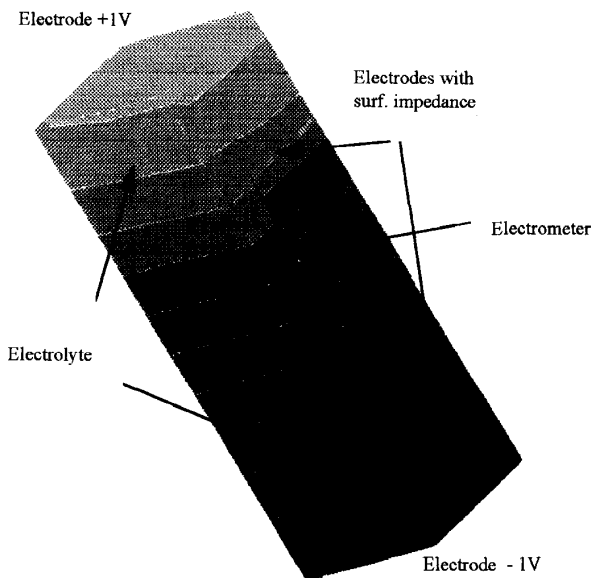Fig. 6. 2D FE Model of the electrometer. Electric potential (f = 1 Hz)

Fig. 7. 3D FE Model of the electrometer. Electric potential (f = 1Hz)

VI. BOUNDARY INTEGRAL EQUATIONS MODEL

The same problem was solved using a BIE model, at the cost of some slight modifications in a standard software [3].

A. Standard formulation

In the electrolyte region $\mathcal{V}$, the conductivity is constant, then (1) becomes a Laplace's equation:

$$\Delta\Phi \equiv 0 \quad \text{on each point of } \mathcal{V} \tag{14}$$

which is equivalent to [10]:

$$\Omega_{\mathcal{V}}(P)\cdot\Phi(P) = -\iint_{\partial\mathcal{V}}\left[\Phi(Q)\frac{\partial G_P}{\partial n}\bigg|_Q - \frac{\partial\Phi}{\partial n}\bigg|_Q G_P(Q)\right]\cdot ds_Q$$

$$\text{on each point } P \text{ of the boundary } \partial\mathcal{V} \text{ of } \mathcal{V} \tag{15}$$

$$\text{with: } G_P(Q) = \frac{1}{4\pi PQ} \qquad \text{Green's function} \tag{16}$$

$$\frac{\partial G_P}{\partial n}\bigg|_Q = \frac{\overrightarrow{PQ}.\bar{n}_Q}{4\pi PQ^3} \tag{17}$$

$$\Omega_{\mathcal{V}}(P) = \iint_{\partial\mathcal{V}}\frac{\partial G_P}{\partial n}\bigg|_Q \cdot ds_Q \quad \sim \text{solid angle} \tag{18}$$

B. Special interface equation

The BIE (15) links together the boundary functions Φ and $\partial\Phi/\partial n$ $(= \bar{\nabla}\Phi\cdot\bar{n})$ and is particularly suitable to take into account the interface equations (3) and (4): when P or Q is on the interface, we obtain a second link between these functions:

$$\Phi(P) = V_0 + \frac{\sigma_1}{\sigma_S}\frac{\partial\Phi}{\partial n}\bigg|_P \quad \Phi(Q) = V_0 + \frac{\sigma_1}{\sigma_S}\frac{\partial\Phi}{\partial n}\bigg|_Q \tag{19}$$

V_0 : inner potential of the electrode

The substitution of this equation in (15) allows to take into account the electrochemical effect on an electrode with a BIE formulation.

C. Non-confined environment

With this boundary integral method, it is also possible to forecast the response of the electrometer to a given electric field $E_0 = -\bar{\nabla}\Phi_0$ in a boundless electrolyte: the results will help us to justify the relative little size of the measurement basin (Fig. 2).

In this case, Φ is not the *total* electric potential, but characterises the perturbation of the electric field:

$$\bar{E} = -\bar{\nabla}(\Phi_0 + \Phi) \tag{20}$$

Φ obeys the Laplace's equation (and the boundary integral equation), but the interface equation (19) turns :

$$\Phi - \Phi_0 = V_0 + \frac{\sigma_1}{\sigma_S}(\frac{\partial\Phi}{\partial n} - E_{0n}) \tag{21}$$

(E_0 is known and Φ_0 will be deduced from it [11])

D. Inner impedance: an equivalent model

The BIE program we used does not accept circuit equations. Therefore, the inductive behaviour of the inside of the electrometer was simulated using an equivalent 3D conduction problem and a fictitious *inductive* electrode :
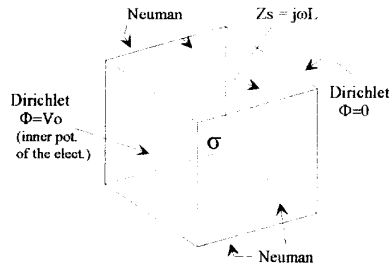
Neuman   Zs = jωL

Dirichlet
Φ=Vo
(inner pot.
of the elect.)   Dirichlet
Φ=0

σ

Neuman

Fig. 8. BIE model for the inner impedance of the electrometer

E. Example of BIEM 3D results.

Electrode with
surface impedance

Source
electrode
f = 1 Hz

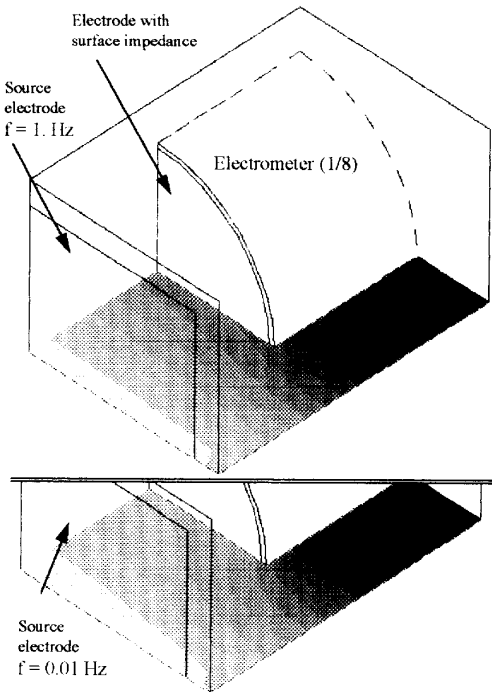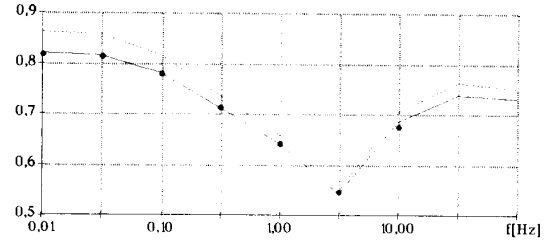Electrometer (1/8)

Source
electrode
f = 0.01 Hz

Fig. 9. 3D BIE Model of the electrometer
Electric potential at z=0. (real part) : influence of the frequency.

VII. COMPARATIVE RESULTS

Fig. 10 shows the excellent agreement between FE and BIE models. So interfacial elements seem to be validated and could be used to model other interface phenomena (§VIII). BIE results for *confined* and *open* space are very similar: we can expect the electrometer to have the same behaviour in the sea as in the measurement basin.

Numerical results are just in correct agreement with measurements (fig. 11). The difference may be due to the very simple circuit model used for the electrochemical effect.

(a) Centre of the electrode, electrolyte-side
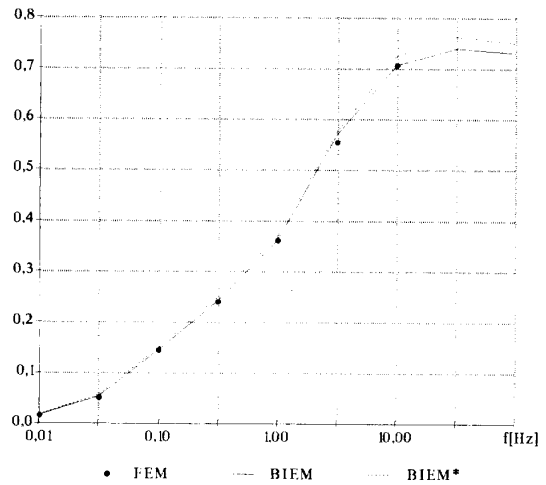
● FEM   —— BIEM   ······ BIEM*

(b) Centre of the electrode, inner-side

Fig. 10. 3D Models of the electrometer : electric potential
comparison FEM / BIEM
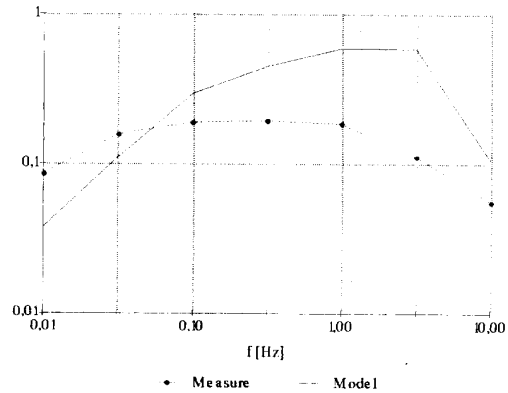and confined / infinite (* : infinite electrolyte)

● Measure   —— Model

Fig. 11. Electrometer : comparison computation/measurement

VIII. EXAMPLE 2 : THERMOELECTRIC SEEBECK EFFECT

In the first example (§III to §VII), we have validated that the general interfacial element can be used in order to take into account direct drops of the unknown (Eq. 4). In this second example we will compute simultaneous normal and tangential interfacial discontinuities. This kind of boundary conditions is find in the thermoelectric Seebeck effect. A classical analysis of this phenomena [12] leads to:

$$(1) \quad \bar{\nabla}(-\sigma\bar{\nabla}\Phi) = 0$$

on the domain with boundary conditions:
- classical continuity, of normal current :

$$(3) \quad (\sigma_2\bar{\nabla}\Phi_2 - \sigma_1\bar{\nabla}\Phi_1)\cdot\bar{n} = 0 \quad \text{and:}$$

- thermoelectric effect :

$$\bar{\nabla}\Phi_1 \wedge \bar{n} - \bar{\nabla}\Phi_2 \wedge \bar{n} = (S_1 - S_2)\bar{\nabla}T \wedge \bar{n} \quad (22)$$

where T is the temperature and S_1, S_2 the thermoelectric powers of each material.

In such a case, the hypothesis H_2 cannot be verified. This problem must be solved by assembling two sets of equations in the general matrix of the problem : after a classic Galerkin projection :

$$\iint_S \gamma_i \sum_j \bar{\nabla}\alpha_j \wedge \bar{n}\Phi_j \cdot ds - \iint_S \gamma_i \sum_k \bar{\nabla}\beta_k \wedge \bar{n}\Phi_k \cdot ds$$
$$= \iint_S \gamma_i(S_1 - S_2)\bar{\nabla}T \wedge \bar{n} \cdot ds \quad (23)$$

and :

$$\iint_S \gamma_m \sum_j \bar{\nabla}\alpha_j \wedge \bar{n}\Phi_j \cdot ds - \iint_S \gamma_m \sum_k \bar{\nabla}\beta_k \wedge \bar{n}\Phi_k \cdot ds = 0 \quad (24)$$

where i ∈ interface of media 1
        m ∈ interface of media 2
        j ∈ volume of media 1
        k ∈ volume of media 2
        α, β, γ are the polynomials defined in Fig. 1.

The discontinuous pseudo-electric potential has been computed [5] in the case of an axisymmetric microscopic dendrite submitted to a vertical thermal gradient (Fig. 12).

Fig. 12. Pseudo electric potential on a dendrite with a vertical thermal gradient

CONCLUSION

A general curvilinear interfacial element has been tested in order to solve three kinds of discontinuities :

a) continuity of tangential gradient and discontinuity of normal gradient in linear interface with a small thickness.

b) continuity of tangential gradient and discontinuity of normal gradient on surface impedant interface.

c) discontinuity of *both* tangential and normal gradients at the interface.

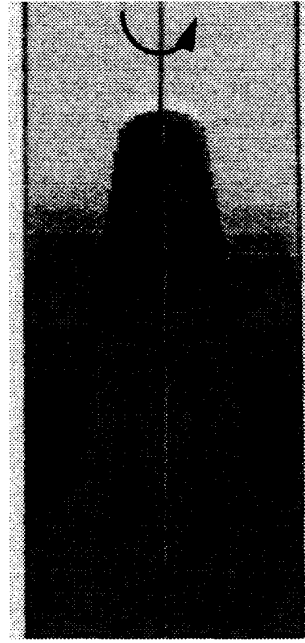This kind of elements are very powerful in order to solve non-natural boundary conditions in FEM.

REFERENCES

[1] Ph. Massé, "Modelling of continuous media methodology and computer aided design of finite element programs," IEEE Trans. Mag., vol. 20, n°5, pp. 1885-1990, 1984.

[2] *FLUX-EXPERT user manual.* DT2I Corp. , 8 ch. des Prèles, ZIRST - 38240 Meylan (France).

[3] L. Krähenbühl, A. Nicolas, L. Nicolas, "The CAD package PHI3D for the computation of electric or magnetic fields in 3D devices," Compel, vol. 9, suppl. A, pp. 185-189.

[4] V. Poulbot, "Contribution à l'étude des champs électriques très basses fréquences en milieu océanique," *Ph. D. Thesis 93-36*, Ecole Centrale de Lyon, France, oct. 1993.

[5] Olivier Laskar, "Phénomènes thermoélectriques et magnéto-hydro-dynamiques en solidification des alliages métalliques," *Ph. D. Thesis*, INP Grenoble, France, jul. 1994.

[6] J.H. Filloux, "Instrumentation and experimental methods for oceanic studies," J.A. Jacobs (ed.), *Geoelectromagnetism 1*, pp. 143-248, 1989.

[7] J. Mosnier, "Dispositif de mesure d'un champ électrique dans un fluide conducteur, et procédé utilisant un tel dispositif," French patent, 84 19577 (FR 2 575 296 - A1), 1986.

[8] U. Rakotosoa, "Appareillage de mesure des très faibles champs électriques en milieu marin. Application à la mise en évidence des signaux électromagnétiques induits dans la mer," *Ph. D. Thesis*, Paris VI, France, 1989.

[9] R. Blanpain, F. Robach, "Procédé et dispositif pour la mesure d'un champ électrique en milieu conducteur," French patent 9102273, 1991.

[10] L. Krähenbühl, A. Nicolas, L. Nicolas, "Contraintes électriques dans une chambre de coupure: une méthode d'analyse tridimensionnelle," RGE, oct. 1989, n°9, pp.44-49.

[11] L. Krähenbühl, "Surface current and eddy current 3D computation using BIE techniques," *Digests 3rd int^al IGTE symposium*, Graz, Austria, sept. 1988.

[12] J.A. Shercliff, "Thermoelectric magnetohydro-dynamics," J. Fluid Mech., vol. 91, part 2, pp. 231-251, 1979.